AGU ADVANCING EARTH AND SPACE SCIENCE

Geophysical Research Letters

RESEARCH LETTER
10.1029/2020GL092206

Analysis of the Anthropogenic and Biogenic NO_x Emissions Over 2008–2017: Assessment of the Trends in the 30 Most Populated Urban Areas in Europe

A. Fortems-Cheiney[1], G. Broquet[1], I. Pison[1], M. Saunois[1], E. Potier[1], A. Berchet[1], G. Dufour[2], G. Siour[2], H. Denier van der Gon[3], S. N. C. Dellaert[3], and K. F. Boersma[4,5]

[1]Laboratoire des Sciences du Climat et de l'Environnement, LSCE-IPSL (CEA-CNRS-UVSQ), Université Paris-Saclay, Gif-sur-Yvette, France, [2]Laboratoire Interuniversitaire des Systèmes Atmosphériques, Université Paris Est Créteil et Université de Paris, Institut Pierre Simon Laplace, Créteil, France, [3]Department of Climate, Air and Sustainability, TNO, Utrecht, the Netherlands, [4]Wageningen University, Meteorology and Air Quality Section, Wageningen, the Netherlands, [5]Royal Netherlands Meteorological Institute, R&D Satellite Observations, De Bilt, the Netherlands

Key Points:

- Over urban areas in Western Europe, OMI confirms the drop of the simulated CHIMERE NO_2 tropospheric vertical column density columns, based on the latest country emission reporting
- Increasing biogenic emissions reconciles CHIMERE and OMI over urban areas in Central Europe and over rural areas, confirming their importance to assess long-term trends
- Over Eastern Europe, our results question emission reductions estimated for particular sectors such as road transport, public power and industrial emissions

Supporting Information:

Supporting Information may be found in the online version of this article.

Correspondence to:

A. Fortems-Cheiney,
audrey.fortems@lsce.ipsl.fr

Citation:

Fortems-Cheiney, A., Broquet, G., Pison, I., Saunois, M., Potier, E., Berchet, A., et al. (2021). Analysis of the anthropogenic and biogenic NO_x emissions over 2008–2017: Assessment of the trends in the 30 most populated urban areas in Europe. *Geophysical Research Letters*, *48*, e2020GL092206. https://doi.org/10.1029/2020GL092206

Received 18 DEC 2020
Accepted 24 APR 2021

Author Contributions:

Conceptualization: A. Fortems-Cheiney
Data curation: E. Potier, A. Berchet, G. Dufour, G. Siour, H. Denier van der Gon, S. N. C. Dellaert, K. F. Boersma
Formal analysis: A. Fortems-Cheiney, G. Broquet, I. Pison, M. Saunois

Abstract We use the OMI-QA4ECV-v1.1 NO_2 tropospheric columns over the 10-year 2008–2017 period to confront satellite-based trends in NO_2 concentrations to those from the state-of-the-art regional chemistry-transport model CHIMERE and to evaluate the bottom-up anthropogenic and biogenic NO_x emissions in Europe. A focus is made for the 30 most populated urban areas in Europe. Over urban areas in Western Europe, except for coastal cities, OMI confirms the drop in the simulated CHIMERE NO_2 tropospheric columns based on the latest country emission official reporting. OMI hardly shows significant negative trends over Central and Eastern Europe urban areas. Increasing biogenic emissions helps reconciling CHIMERE and OMI trends over urban areas in Central Europe and over rural areas, confirming the importance of accounting for non-anthropogenic emissions to assess long-term trends. Over Eastern Europe, our results question emission reductions estimated for particular sectors and in particular the road transport, public power, and industrial emissions.

Plain Language Summary We evaluate anthropogenic and biogenic nitrogen oxides (NO_x) emissions in Europe by analyzing nitrogen dioxide (NO_2) 10-yr trends both from satellite observations and from simulations. A focus is made for the 30 most populated urban areas in Europe, particularly exposed to air pollution. The similarities and discrepancies between simulations and satellite observations indeed must be investigated. It is important particularly for policy implications as anthropogenic emissions are based on the official reported emissions form the basis for negotiation on emission reductions in the EU and are used to assess if countries meet their agreed emission ceilings.

1. Introduction

Mainly emitted by road traffic, thermal power plants and industrial activities and produced in the atmosphere by the oxidation of nitric oxide (NO), nitrogen dioxide (NO_2) is one of the major air pollutants with adverse impact on health (Costa et al., 2014; Khaniabadi et al., 2017). It is partly contributing to the 400,000 premature deaths attributed to air pollution in Europe in 2018 (EEA, 2020). NO_2 is therefore one of the most regulated air quality pollutants, with a limit of 40 $\mu g/m^3$ for the annual mean concentrations set both by the "2008/50/EC Directive on ambient air quality and cleaner air for Europe" and by the air quality guidelines of the World Health Organization (WHO). NO_2 is also a precursor of tropospheric ozone and particulate matter including nitrates. Deposition of nitrogen compounds like nitrates leads to eutrophication of ecosystems (Stevens et al., 2018). Therefore, NO_2 is of great interest due to its important role in many atmospheric processes with strong implications for air quality, health, climate change, and ecosystems.

Due to the lack of independent constraints on large scale budgets, the quantification of nitrogen oxides ($NO_x = NO + NO_2$) emissions in bottom-up (BU) inventories is difficult. This quantification is particularly sensitive to emissions factors (to be applied to activity levels), which are still highly uncertain, with uncertainties that can reach 50%–200% (Kuenen and Dore, 2019) and which can even be biased sometimes (as illustrated by the "DieselGate" Brand, 2016). The atmospheric monitoring of NO_x emissions based on in-situ measurements is also challenging. Air quality networks provide measurements of NO_x mixing ratios,

Writing – original draft: A. Fortems-Cheiney, G. Broquet, I. Pison, M. Saunois
Writing – review & editing: A. Fortems-Cheiney, G. Broquet, I. Pison, M. Saunois, E. Potier, A. Berchet, G. Dufour, G. Siour, H. Denier van der Gon, S. N. C. Dellaert, K. F. Boersma

representative of the street scale to local scale levels, which are difficult to properly use to quantify emissions at the city to regional scales.

Satellite observations of NO_2 tropospheric columns are an effective proxy for NO_x emissions in polluted areas (Lamsal et al., 2015; Li & Wang, 2019; Miyazaki et al., 2017; Silvern et al., 2019). They allow the study of long-term variations for various regions of the world (Lamsal et al., 2015; Miyazaki et al., 2017; Schneider et al., 2015; van der A et al., 2008). Space-based observations from the Global Ozone Monitoring Experiment GOME (Burrows et al., 1999) and GOME-2 (Munro et al., 2016), from the SCanning Imaging Absorption spectroMeter for Atmospheric CHartographY SCIAMACHY (Bovensmann et al., 1999; Burrows et al., 1995) and from the Ozone Monitoring Instrument OMI showed that there were reductions in NO_2 levels since the late 1990 over Western Europe (Castellanos and Boersma, 2012; Curier et al., 2014; Georgoulias et al., 2019; Krotkov et al., 2016; Schneider et al., 2015; van der A et al., 2008). However, in 2017, 16 of the EU Member States and four other reporting countries still recorded near ground NO_2 concentrations whose annual mean was above the recommended limit of 40 $\mu g/m^3$ at the air quality stations within large urban areas (EEA, 2019), where populations are particularly exposed.

The previously cited studies analyzed the trends in NO_2 tropospheric vertical column density (TVCD) observed by satellite observations over Europe. However, the causes of these trends (i.e., trends in meteorology, atmospheric general composition, chemistry, emissions) are rarely investigated and few studies properly compared them to simulated concentrations based on chemistry-transport model (CTM; Curier et al., 2014). Such studies would be very useful since CTM simulations based on BU inventories can help determining the main processes controlling concentrations trends, and especially the impact of changes in surface emissions. Our study presents the first comparison of simulated and observed NO_2 TVCD trends over 10 years, at a rather high resolution (0.5° × 0.5°) over Europe, based on the latest emissions reported by countries. In the following, we use the regional model CHIMERE, which is a CTM widely used to monitor air quality (Blond et al., 2007; Cholakian et al., 2019; Ciarelli et al., 2019; Mailler et al., 2017; Menut et al., 2013; Menut, Bessagnet, Siour, et al., 2020; Terrenoire et al., 2015), and part of the seven state-of-the-art CTMs used in the operational ensemble of the Copernicus Atmosphere Monitoring Service (CAMS) regional services. In our approach, the emission input for the CHIMERE model is based on the latest country emission reporting to European Monitoring and Evaluation Program (EMEP)/Center on Emission Inventories Projection (CEIP) spatially and temporally disaggregated in the new TNO-GHGco-v2 inventory (Denier van der Gon, 2020). Compared with other UV-Vis instruments providing a long archive of NO_2 observations, OMI has the highest spatial resolution and least degradation (Levelt et al., 2018; Schenkeveld et al., 2017). As a result, we use the OMI-QA4ECV-v1.1 NO_2 TVCDs (Boersma et al., 2017, 2018) over the 10-year 2008–2017 period to confront the satellite-based trends in NO_2 concentrations to those from CHIMERE CTM in order to evaluate the impact of the bottom-up anthropogenic and biogenic NO_x emission trends, particularly over the 30 most populated urban areas in Europe (large cities and their suburbs).

2. Data and Method

We use the regional CTM CHIMERE (Menut et al., 2013), driven by the PYVAR-CHIMERE system (Fortems-Cheiney et al., 2019) to simulate NO_2 TVCD corresponding to the satellite OMI-QA4ECV-v1.1 data (Boersma et al., 2017). Then we compute and compare the observed and simulated trends for the last 10-year period including the last year reported by countries to EMEP/CEIP, from January 2008 to December 2017.

2.1. CHIMERE Set-Up

The CHIMERE reference simulation has been performed with the following set-up. CHIMERE is run over a 0.5° × 0.5° regular grid and 17 vertical layers, from the surface to 200 hPa, with 8 layers within the first two kilometers. The domain includes 101 (longitude) × 85 (latitude) grid-cells (15.25°W–35.75°E; 31.75–74.25°N) and covers Europe (Figure 1). CHIMERE is driven by the European Center for Medium-Range Weather Forecasts (ECMWF) meteorological forecast (Owens & Hewson, 2018). The chemical scheme used in CHIMERE is MELCHIOR-2, with more than 100 reactions (CHIMERE, 2017; Lattuati, 1997), including 24 for inorganic chemistry. Climatological values from the LMDZ-INCA global model (Szopa et al., 2008)

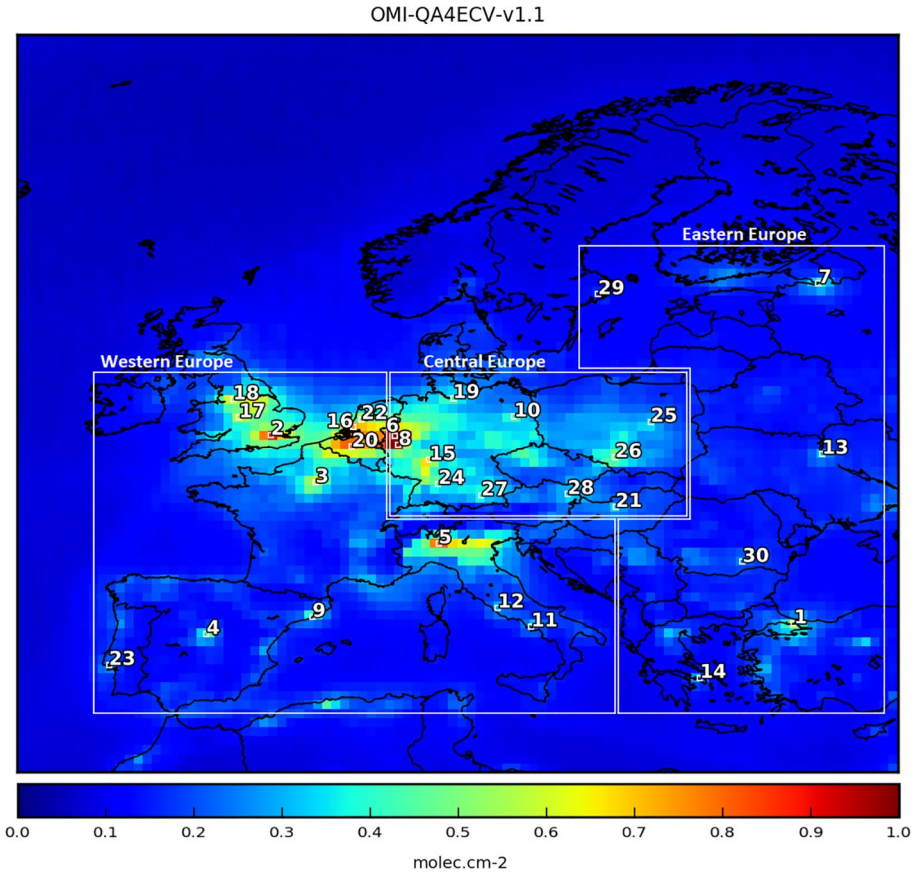

Figure 1. Mean observed tropospheric columns by OMI-QA4ECV-v1.1 for the 10-year 2008–2017 period, in 10^{16} molec. cm^{-2}. The 30 urban areas are numbered from the most to the least populated according to MAW (2020) and are listed in Table S1. The three white boxes represent Western, Central and Eastern Europe.

are used to prescribe concentrations at the lateral and top boundaries and the initial atmospheric composition in the domain. Considering the NO_2 short lifetime, we do not consider its import from outside the domain: its boundary conditions are set to zero. Nevertheless, we take into account peroxyacetyl nitrate (PAN), the NO_x reservoir, to transport NO_x at the large scale accurately.

For anthropogenic NO_x emissions between 2008 and 2017, we use the new TNO-GHGco-v2 gridded inventory. This version is an update of the TNO inventory distributed in Kuenen et al., (2014) and in Super et al., (2020). This inventory is based on the last EMEP/CEIP official country reporting for air pollutants, done in 2019. It maps emissions at a 6 × 6 km^2 horizontal resolution. Annual and national budgets are disaggregated in space based on proxies of the different sectors (Kuenen et al., 2014). Temporal disaggregation is based on temporal profiles provided per Gridded Nomenclature For Reporting (GNFR) sector code with typical month to month, weekday to week-end and diurnal variations. Following the Generation of European Emission Data for Episodes (GENEMIS) recommendations (Aumont et al., 2003; Kurtenbach et al., 2001), we speciated the TNO-GHGco-v2 NO_x emissions as 90% of NO, 9.2% of NO_2, and 0.8% of nitrous acid (HONO). The TNO-GHGco-v2 inventory has been aggregated at the 0.5° × 0.5° horizontal resolution of the CHIMERE grid. Biogenic soil NO emissions are calculated from the MEGAN model (Guenther et al., 2006). Lightning NO_x fluxes, which impact on NO_2 concentrations is very small in Europe even in summer (Menut, Bessagnet, Mailler, et al., 2020), are not accounted for in this study. Fire emissions are also not accounted in our study. We assume they only slightly contribute to the NO_x total emissions and to the 10-year NO_2 trends. The annual budgets for anthropogenic and biogenic emissions over our total domain are respectively 17,610 $ktNO_2$ and 273 $ktNO_2$ in 2008. The contribution of the anthropogenic emissions to the NO_x total continental emissions in 2008 is shown in Figure S1.

Table 1
Description of the CHIMERE Simulations Performed in This Study

Name	Objective of the simulation	NO_x anthropogenic emissions	NO biogenic emissions
reference	Baseline scenario	TNO-GHGco-v2	MEGAN
A	Sensitivity to meteorology	TNO-GHGco-v2 constant at the 2008 levels	MEGAN constant at the 2008 levels
B	Sensitivity to biogenic emissions	TNO-GHGco-v2 constant at the 2008 levels	MEGAN
C	Sensitivity to increased biogenic emissions	TNO-GHGco-v2	MEGAN multiplied by 5

As the NO_2 TVCD 10-year trends simulated by CHIMERE could be driven by anthropogenic and biogenic NO_x emissions and by meteorology, different sensitivity tests have been performed to assess their impacts on the 10-year NO_2 TVCD trends (Table 1). To assess the relative weight of meteorology on the simulated NO_2 TVCD trends, we performed the sensitivity test A keeping the anthropogenic emissions and the biogenic emissions constant at 2008 levels. To assess the relative weight of the biogenic emissions, we performed the sensitivity test B keeping the anthropogenic emissions constant at 2008 levels. However, Visser et al. (2019) found that the MEGAN model underestimates soil NO_x emissions by a factor of 5–7, as it only contains natural soil NO_x emissions and not agricultural enhanced emissions due to fertilization. We then performed the sensitivity test C, with MEGAN biogenic NO_x emissions increased by a factor 5, to assess the impact of increased biogenic NO_x emissions on TVCD long-term trends over Europe. It should be noted that this scaling up of the MEGAN pattern is a simplification: the agriculturally enhanced soil NO_x emissions should be concentrated in agricultural hotspots.

2.2. OMI-QA4ECV-v1.1 Observations

OMI, a near-UV/Visible nadir solar backscatter spectrometer, was launched onboard EOS Aura in July 2004. It flies on a 705 km altitude sun-synchronous orbit that crosses the Equator at 13:40 LT. Our OMI-QA4ECV-v1.1 data selection follows the criteria of the data quality statement (Boersma et al., 2017). For this data set, we select data for which:

- the processing error flag equals 0 for a pixel,
- the solar zenith angle is lower than 80°,
- the snow ice flag is lower than 10 or equal to 255,
- the ratio of tropospheric AMF over geometric AMF is higher than 0.2 to avoid situations in which the retrieval is based on very low (relative) tropospheric air mass factors,
- the cloud fraction is lower than 0.25.

As the spatial resolution of the OMI data of 13×24 km^2 at nadir is finer than that of the chosen CHIMERE model grid, the selected OMI TVCD are aggregated into "super-observations." To make comparisons between simulations and satellite observations, the averaging kernels (AK) must be taken into account (Eskes & Boersma, 2003). In order to associate the super-observations to a real AK, these super-observations are taken as the observations (TVCD and AK) corresponding to the median of the OMI TVCD within the $0.5° \times 0.5°$ model grid-cell and within the CHIMERE physical time step of about 5/10 min.

The average of these super-observations of OMI-QA4ECV-v1.1 NO_2 TVCD, binned at 0.5° resolution, over the 10-year 2008–2017 period in Europe are shown in Figure 1. The European domain is separated into three boxes representing Western, Central and Eastern Europe. It should be noted that countries of Southern Europe (Italy, Spain, and Portugal) are labeled "Western" hereafter. OMI shows wide patterns of strong NO_2 values higher than 6×10^{15} molec.cm^{-2} over Western and Central Europe, particularly over southeastern UK, northeastern France, northern Italy, Benelux and Germany. It also shows isolated hotspots, with values often higher than 4×10^{15} molec.cm^{-2}, representative of populated urban areas (Schneider et al., 2015). For the following, we numbered the 30 most populated urban areas in our domain covering Europe (Figure 1 and Table S1) according to the Major Agglomerations of the World (MAW) website (www.citypopulation.de, MAW, 2020).

2.3. Time Series Analysis Method

We compute the monthly averages of the OMI-QA4ECV-v1.1 super-observations and of the corresponding simulation with CHIMERE. Monthly biogenic NO and anthropogenic NO_x emissions have also been computed. From these monthly fields, we calculate the deseasonalized monthly time series using the average-percentage method, as in Dufour et al. (2018). A climatological index is calculated over the 10-year period. It is then applied to the monthly time series to remove the seasonal component and obtain the deseasonalized time series. The Theil–Sen estimator (Sen, 1968) and the non-parametric Mann-Kendall test (Kendall, 1975) are used to estimate the linear trend. All the linear trends presented in this study are computed based on the deseasonalized time series. These trends are given in %/yr. The uncertainty on these trends corresponds to the 95% confidence interval and is also given in %/yr in the following. A trend is considered significant if the change in NO_2 TVCD exceeds their uncertainty. In this study, this is equivalent to selecting the trends with a p value lower than 0.05.

3. Results and Discussion

3.1. A Strong NO_2 Decrease Simulated by the CHIMERE Reference Over Western Europe

Over Western Europe, the CHIMERE reference simulated NO_2 TVCDs show significant negative trends, up to −4%/yr (Figure 2). It can be seen that these significant negative trends mainly apply to large parts of the countries Portugal, Spain, UK, France, Italy, Belgium, and the Netherlands, thus suggesting that the NO_2 TVCDs in these countries located in our Western Europe domain have significantly decreased since 2008. The areas with significant negative trends in other European countries are much smaller.

The decrease of the NO_2 TVCDs is mainly found over polluted areas defined as areas where annual anthropogenic NO_x emissions are higher than 5ktNO_2 in 2008 (Figure S1a)- and particularly over urban agglomerations. The trends for the most populated urban areas in our domain shown in Figure 3 are indeed significantly negative for 26 urban areas out of 30. Over Western Europe, rural areas -defined as areas where annual anthropogenic NO_x emissions do not exceed 5ktNO_2 in 2008 (Figure S1a)- show significant trends but smaller than over polluted areas. Over Central and Eastern Europe, rural areas do not show significant trends.

3.2. OMI Confirms the Drop in NO_2 TVCDs Shown by CHIMERE Over Most of the Urban Areas in Western Europe

OMI TVCDs also show significant negative trends over Western Europe, mainly focused on polluted areas (Figure 2d). Zara et al., (2021) also found that the strongest trends in Europe occur for the most polluted regions. OMI confirms the drop in NO_2 TVCDs simulated by CHIMERE over nine urban areas in Western Europe: Madrid, Manchester, Birmingham, Barcelona, Paris, Brussels, Amsterdam, Milan and Rome (Figure 3a), demonstrating that the urban air quality in these agglomerations has been significantly improved since 2008. In these nine urban areas, the range of trend estimates from OMI is similar to that from CHIMERE (e.g., −3.3 ± 2.0%/yr for OMI against −2.9 ± 2.0%/yr for CHIMERE for Paris, −3.8 ± 1.1%/yr for OMI against −3.3 ± 1.1%/yr for CHIMERE for Rome, Figure 3a). It is interesting to note that for the coastal cities London in UK, for Lisbon in Portugal, for Rotterdam in the Netherlands and for Naples in Italy, we get negative trends in the OMI data but that these trends are, however, not diagnosed as being significant (Figure 3a). Even though our super-observations are taken as the median of the OMI TVCD within the 0.5° × 0.5° model grid-cell, they could be impacted by a problem of representativity as parts of the grid-cells are covered by the sea. This might explain the lack of significance in the analysis of the trends for these cities. Actually, significant negative trends were diagnosed with OMI oversampled data and ground stations over Rotterdam (Zara et al., 2021). Over Western Europe, it is also interesting to note that OMI does not confirm the drop in the NO_2 TVCD columns over rural areas (Figure 2d).

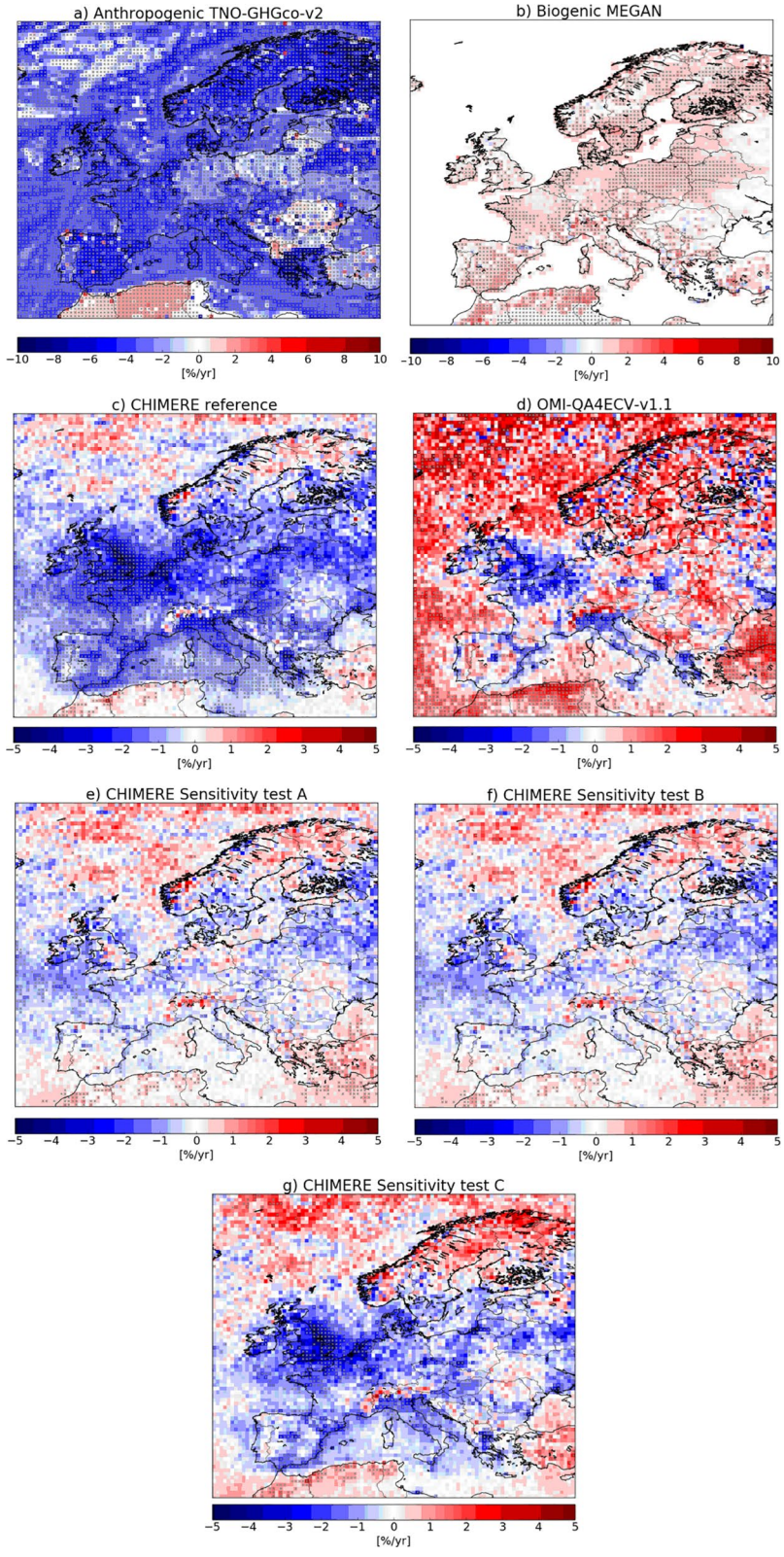
a) Anthropogenic TNO-GHGco-v2
b) Biogenic MEGAN
c) CHIMERE reference
d) OMI-QA4ECV-v1.1
e) CHIMERE Sensitivity test A
f) CHIMERE Sensitivity test B
g) CHIMERE Sensitivity test C
[%/yr]

3.3. OMI Disproves the Drop in NO_2 TVCDs Shown by CHIMERE Over Most of the Urban Areas in Central and Eastern Europe

Simulated CHIMERE NO_2 TVCDs present a significant negative trend for the most populated urban areas located in Central and Eastern Europe, except for the Ruhr area, Munich, Vienna and Stockholm (Figures 3b and Figure 3c). By contrast, in these regions, the OMI satellite observations show significant negative trends only over the Ruhr area (−2.9 ± 1.7%/yr), Frankfurt (−1.5 ± 1.3%/yr) and Kiev (−0.95 ± 0.7%/yr). For the other urban areas located in Central and Eastern Europe, including many German urban areas (e.g., Cologne, Stuttgart, Munich and Berlin), OMI data show negative trends that are not significant (Figure 3b). Over Istanbul, as seen in Zara et al. (2021), OMI TVCDs show a significant positive trend whereas CHIMERE TVCDs show a negative one (+2.8 ± 2.0%/yr for OMI against −0.9 ± 0.8%/yr for CHIMERE). It is finally also interesting to note that the insignificant OMI NO_2 TVCD trends over rural areas in Eastern Europe are consistent with the CHIMERE simulated TVCD trends. This is also consistent with the study of Krotkov et al. (2016) for the period 2005–2015.

3.4. Questioning the Discrepancies Between OMI and CHIMERE NO_2 TVCD Trends in Central and Eastern Europe Urban Areas: Impact of Biogenic Emissions and Uncertainties in the Emission Inventories

The sensitivity test A demonstrates the negligible influence of meteorology variations on the NO_2 TVCD trends (Figure 2e), as already noticed by Castellanos and Boersma (2012) and by Krotkov et al. (2016). The lack of significant trends in the OMI-QA4ECV-v1.1 NO_2 satellite observations over the in Central and Eastern Europe urban areas (Figures 2d and Figure 3) therefore question:

(a) the magnitude of the biogenic emissions, as the MEGAN module does not capture agriculturally enhanced soil NO_x emissions by design (Guenther et al., 2006),
(b) the emission reductions estimated for particular sectors over these regions by the TNO-GHGco-v2 inventory, which is based on the last official declarations by countries.

3.4.1. Questioning the Magnitude of the Biogenic Emissions

The biogenic emissions calculated by CHIMERE over Europe show significant positive trends over the 2008–2017 period, up to +2%/yr (Figure 2b). This is relatively small compared to the trends of anthropogenic NO_x emissions, up to −10%/yr (Figure 2a). In addition, the relative contribution of biogenic emissions to total NO_x emissions is small (Figure S1b). With the sensitivity test B, the NO_2 TVCD trends are similar to those of the sensitivity test A, with small and insignificant trends almost everywhere in Europe (Figure 2f). In our reference simulation, the biogenic emissions thus only slightly contribute to the trend of NO_x total emissions over Europe, even over rural areas. However, with higher biogenic emissions as estimated by Visser et al. (2019) in the sensitivity test C, the CHIMERE trends are dampened in many locations. It helps reconciling CHIMERE and OMI trends over Cologne, Hamburg and Berlin in Central Europe, where CHIMERE trends become insignificant (Figure 3b). It also helps reconciling CHIMERE and OMI trends over rural areas (Figure 2g), confirming the importance of accounting for non-anthropogenic emissions to assess TVCD long-term trends (Silvern et al., 2019). Nevertheless, as the CHIMERE trends remain similar, this test with increased NO_x biogenic emissions does not reconcile CHIMERE and OMI over coastal cities in Western Europe (e.g., Lisbon, London, Rotterdam, and Naples, Figure 3a) and over urban areas in Eastern Europe (e.g., Athens, Bucharest, and St-Petersburg, Figure 3c).

Figure 2. Ten-year trends calculated from monthly deseasonalized time series of NO_x (a) TNO-GHGco-v2 anthropogenic emissions and (b) biogenic emissions calculated from the MEGAN model. 10-year trends calculated from monthly deseasonalized time series of NO_2 TVCD (c) simulated by the CHIMERE reference simulation, (d) observed by OMI-QA4ECV-v1.1, (e) simulated by CHIMERE with biogenic and anthropogenic emissions constant at their 2008 levels in the sensitivity test A, (f) simulated by CHIMERE with anthropogenic emissions constant at their 2008 levels in the sensitivity test B and (g) simulated by CHIMERE with biogenic emissions increased by a factor 5 in the sensitivity test C, for the period 2008–2017. Pixels with significant trend are shown with a cross symbol. Units are %/yr. Note that the scale for the emission trends in (a) and (b) are different from the other figures. TVCD, tropospheric vertical column density.

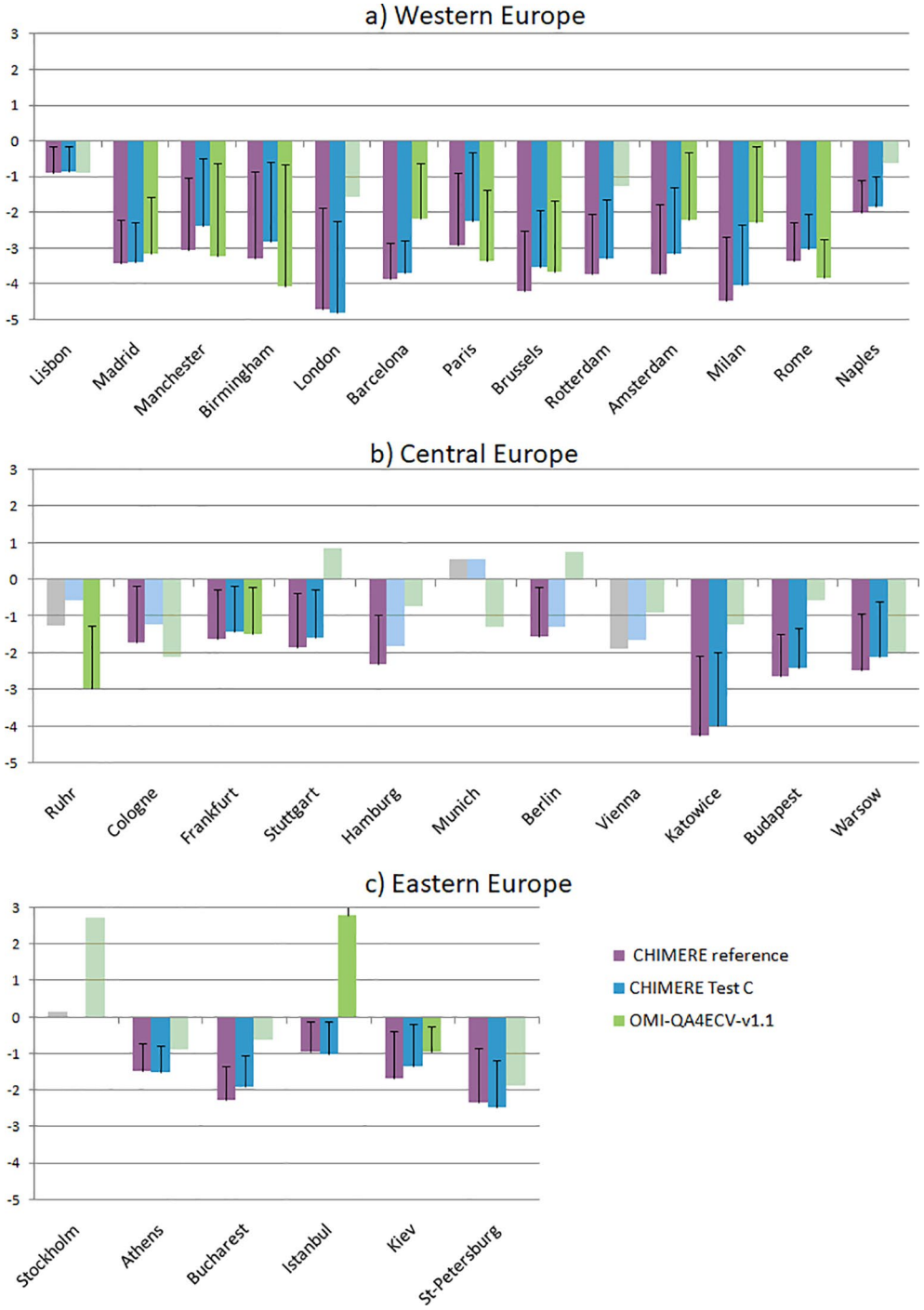

Figure 3. Ten-year trends of NO_2 TVCD simulated by the CHIMERE reference (in purple), by CHIMERE with the sensitivity test C (in blue) and observed by OMI-QA4ECV-v1.1 (in green), for the 30 most populated urban areas in our domain shown from west to east in (a) Western, (b) Central, and (c) Eastern Europe. Significant trends are shown in dark color with their corresponding uncertainties. Units are %/yr. TVCD, tropospheric vertical column density.

3.4.2. Questioning the Anthropogenic Emission Reductions

Figure S2 presents the contribution of six sectors to the trends in total anthropogenic NO_x emissions in the TNO-GHGco-v2 inventory, from 2008 to 2017. The contribution per sector (i) has been calculated as:

$$\text{contribution}(i) = \frac{(\text{10yr trend sectoral } i \text{ emissions}) \text{ x } (\text{sectoral } i \text{ emissions in 2008})}{(\text{10yr trend total emissions}) \text{ x } (\text{total emissions in 2008})} \quad (1)$$

where 10-year trend sectoral *i* and 10-year trend total emissions are the trends in sector *i* emissions and in total emissions over 2008–2017, respectively; and sectoral *i* emission 2008 and total emissions 2008 are the annual emissions in 2008 for sector i and for total emissions, respectively.

Note that a positive contribution means that the sectoral emissions are contributing to the either positive or negative trend in total NO_x emissions. A negative contribution indicates that the sign of the trend in the sectoral emissions is opposite to the trend in total NO_x emissions. Road transport diesel (RTD) emissions (Figure S2b) contribute the most to the negative trends in anthropogenic NO_x emissions (Figure S2a). With lower NO_x emissions than RTD but a higher negative trend of its emissions, the Road transport Gasoline (RTG) emissions also strongly contribute (Figure S2c). Industrial (Figure S2d), public power (Figure S2e) and residential emissions (Figure S2f) can contribute to the negative trends in anthropogenic NO_x emissions. For example, the contribution of the energy sector is of about 55% in Budapest. Contributions of emissions from other sectors, such as shipping (Figure S2g) to the trend in anthropogenic NO_x emissions are small.

Different studies found that the emissions factors used in inventories for Road Transport Diesel (RTD) emissions and their long-term trends compared poorly with the real world (Beevers et al., 2012; EEA, 2016; ICCT, 2014). In the TNO-GHGco-v2 inventory, this issue is partly accounted as they use « real-driving conditions » RTD emissions from the EMEP/EEA Guidebook (Ntziachristos & Samaras, 2019), based on the Emisia COPERT data set (https://www.emisia.com/utilities/copert-data/). They use the Emisia data set mainly to spatially distribute the emissions. However, the total emissions by country are taken from the official reported data. These are often based on Emisia/COPERT data but it could differ by country. RTD emissions contribute more to the trend in total NO_x emissions (Figure S2b) over Central and Eastern Europe than over Western Europe. For example, the contribution of RTD emissions to the trend in total NO_x emissions is of 70% for Bucharest against 35% for London. It could partly explain the discrepancies between OMI-QA4ECV-v1.1 and CHIMERE over these parts of Europe.

It is also interesting to note that emissions from the public power and industry sectors increase since 2008 in the TNO-GHGco-v2 inventory for some urban areas located in Central and Eastern Europe. For example, industrial emissions have increased in Stuttgart and in Frankfurt from 2008 to 2017. Emissions from the energy sector have increased over Hamburg, Stuttgart, Frankfurt, Munich and Warsaw urban areas (Figure S2). The increase in Hamburg is due to the commissioning of coal-fired power station of Moorburg-Hamburg in 2015. The increase in Stuttgart is also due to electricity production from coal. Negative contributions to the trends in total NO_x emissions from residential (Figure S2f) and road transport gasoline emissions (Figure S2c) are also estimated over Warsaw and Bucharest. An under-estimation of the trends associated with these anthropogenic activities could explain the discrepancies between OMI-QA4ECV-v1.1 and CHIMERE trends over these urban regions.

Finally, contributions from other sectors such as shipping could be underestimated. The trends in NO_2 emissions from shipping prior to 2014 are uncertain because activity data derived from the messages broadcast by vessel's Automatic Identification Systems (AIS) data (IMO, 2000; Jalkanen et al., 2009) were not yet used to estimate the emissions. These emissions and their trends may influence especially coastal cities. This could explain the discrepancies between OMI-QA4ECV-v1.1 and CHIMERE particularly over Lisbon, London, Rotterdam, and Naples.

4. Conclusions

The anthropogenic emissions based on the official reported emissions form the basis for negotiation on emission reductions in the EU and are used to assess if countries meet their agreed emission ceilings (EU Directive 2016/2284). An inventory based on these reported emissions is used as input for CHIMERE CTM to simulate NO2 TVCDs, which are then comparable to OMI data. Over urban areas in Western Europe, OMI confirms the drop of the simulated CHIMERE NO_2 TVCD columns, based on the latest country emission reporting. Over Eastern Europe, our results question emission reductions estimated for particular sectors such as road transport, public power and industrial emissions: this decrease may be less than official reported NO_x emissions suggest. Increasing the biogenic emissions provided as input of CHIMERE reconciles the simulated NO_2 TVCDs and OMI data over urban areas in Central Europe and over rural areas. This confirms the importance of biogenic emissions to assess NO_2 long-term trends. The discrepancies between our CHIMERE simulation and the OMI observations should be further investigated because of the policy implications. Further work should be done to quantify diffuse and partly natural NO_x sources (soil emissions over agricultural areas, lightning, fires and the ubiquitous NO_2 background). The TROPOspheric Monitoring Instrument (TROPOMI) on board the Copernicus Sentinel-5 Precursor (S5P) satellite currently measures NO_2 TVCDs at an unprecedented spatial resolution (3.5×5.5 km^2 since August 6, 2019), which will improve the atmospheric monitoring of emissions over urban areas, offering the prospect of a more precise estimate of NO_2 trends over the current decade and making it an important tool for studying urban air pollution.

Conflict of Interests

The authors declare that they have no conflict of interest.

Data Availability Statement

OMI QA4ECV NO_2 product can be found here: www.qa4ecv.eu and http://temis.nl/qa4ecv/no2.html. The OMI NO_2 data set is linked to a digital object identifier (DOI) (http://doi.org/10.21944/qa4ecv-no2-omi-v1.1, Boersma et al., 2017). The CHIMERE code is available here: www.lmd.polytechnique.fr/chimere/, (Mailler et al., 2017; Menut et al., 2013). The TNO-GHGco-v2 inventory (Denier van der Gon, 2020; Super et al., 2020) is available upon request from TNO (contact: Hugo Denier van der Gon, hugo.deniervandergon@tno.nl).

Acknowledgments
A large part of the development and analysis were conducted in the frame of the H2020 VERIFY project, funded by the European Commission Horizon 2020 research and innovation programme, under agreement number 776810. We wish to thank all the persons involved in the preparation, coordination and management of this project. This work was also supported by the CNES (Centre National d'Etudes Spatiales), in the frame of the TOSCA ARGOS project. This work was granted access to the HPC resources of TGCC under the allocations A0070102201 made by GENCI. Finally, we wish to thank F. Marabelle (LSCE) and his team for computer support.

References

Aumont, B., Chervier, F., & Laval, S. (2012). Contribution of HONO sources to the $NO_x/HO_x/O_3$ chemistry in the polluted boundary layer. *Atmospheric Environment*, *37*(4):487–498.

Beevers, S. D., Westmoreland, E., de Jong, M. C., Williams, M. L., & Carslaw, D. C. (2012). Trends in NO_x and NO_2 emissions from road traffic in Great Britain. *Atmospheric Environment*, *54*, 107–116. https://doi.org/10.1016/j.atmosenv.2012.02.028

Blond, N., Boersma, K. F., Eskes, H. J., van der A, R. J., Van Roozendael, M., De Smedt, I., et al. (2007). Intercomparison of SCIAMACHY nitrogen dioxide observations, in situ measurements and air quality modeling results over Western Europe. *Journal of Geophysical Research*, *112*, D10311. https://doi.org/10.1029/2006JD007277

Boersma, K. F., Eskes, H., Richter, A., De Smedt, I., Lorente, A., Beirle, S., et al. (2017). *QA4ECV NO_2 tropospheric and stratospheric vertical column data from OMI (Version 1.1) [Data set]*. Royal Netherlands Meteorological Institute (KNMI). https://doi.org/10.21944/qa4ecv-no2-omi-v1.1

Boersma, K. F., Eskes, H. J., Richter, A., De Smedt, I., Lorente, A., Beirle, S., et al. (2018). Improving algorithms and uncertainty estimates for satellite NO_2 retrievals: Results from the quality assurance for the essential climate variables (QA4ECV) project. *Atmospheric Measurement Techniques*, *11*, 6651–6678. https://doi.org/10.5194/amt-11-6651-2018

Bovensmann, H., Burrows, J. P., Buchwitz, M., Frerick, J., Noël, S., Rozanov, V. V., et al. (1999). SCIAMACHY: Mission objectives and measurement modes. *Journal of the Atmospheric Sciences*, *56*, 127–150. https://doi.org/10.1175/1520-0469(1999)056<0127:smoamm>2.0.co;2

Brand, C. (2016). Beyond "Dieselgate": Implications of unaccounted and future air pollutant emissions and energy use for cars in the United Kingdom. *Energy Policy*, *97*, 1–12. https://doi.org/10.1016/j.enpol.2016.06.036

Burrows, J. P., Hölzle, E., Goede, A. P. H., Visser, H., & Fricke, W. (1995). SCIAMACHY-scanning imaging absorption spectrometer for atmospheric chartography. *Acta Astronautica*, *35*, 445–451. https://doi.org/10.1016/0094-5765(94)00278-T

Burrows, J. P., Weber, M., Buchwitz, M., Rozanov, V., Ladstätter-Weißenmayer, A., Richter, A., et al. (1999). The Global Ozone Monitoring Experiment (GOME): Mission concept and first scientific results. *Journal of the Atmospheric Sciences*, *56*, 151–175. https://doi.org/10.1175/1520-0469(1999)056<0151:TGOMEG>2.0.CO;2

Castellanos, P., & Boersma, K. F. (2012). Reductions in nitrogen oxides over Europe driven by environmental policy and economic recession. *Scientific Reports*, *2*. https://doi.org/10.1038/srep00265

CHIMERE. (2017). *Documentation*. Retrieved from https://www.lmd.polytechnique.fr/chimere/docs/CHIMEREdoc2017.pdf

Cholakian, A., Beekmann, M., Coll, I., Ciarelli, G., & Colette, A. (2019). Biogenic secondary organic aerosol sensitivity to organic aerosol simulation schemes in climate projections. *Atmospheric Chemistry and Physics*, *19*, 13209–13226. https://doi.org/10.5194/acp-19-13209-2019

Ciarelli, G., Theobald, M. R., Vivanco, M. G., Beekmann, M., Aas, W., Andersson, C., et al. (2019). Trends of inorganic and organic aerosols and precursor gases in Europe: Insights from the EURODELTA multi-model experiment over the 1990-2010 period. *Geoscientific Model Development*, *12*, 4923–4954. https://doi.org/10.5194/gmd-12-4923-2019

Costa, S., Ferreira, J., Silveira, C., Costa, C., Lopes, D., Relvas, H., et al. (2014). Integrating health on air quality assessment-review report on health risks of two major European outdoor air pollutants: PM and NO_2. *Journal of Toxicology and Environmental Health, Part B*, *17*(6), 307–340. https://doi.org/10.1080/10937404.2014.946164

Curier, R. L., Kranenburg, R., Segers, A. J. S., Timmermans, R. M. A., & Schaap, M. (2014). Synergistic use of OMI NO_2 tropospheric columns and LOTOS–EUROS to evaluate the NOx emission trends across Europe. *Remote Sensing of Environment*, *149*, 58–69. https://doi.org/10.1016/j.rse.2014.03.032

Denier van der Gon, H. (2020). *VERIFY deliverable D2.2 "second high resolution emission data 2005-2017"*. Retrieved from https://verify.lsce.ipsl.fr/index.php/repository/public-deliverables/wp2-verification-methods-for-fossil-co2-emissions/d2-2-second-high-resolution-emission-data-2005-2017

Directive, (EU). (2016). *2016/2284 of the European Parliament and of the Council of 14 December 2016 on the reduction of national emissions of certain atmospheric pollutants, amending Directive 2003/35/EC and repealing Directive 2001/81/EC [Data set]*. Retrieved from http://data.europa.eu/eli/dir/2016/2284/oj

Dufour, G., Eremenko, M., Beekmann, M., Cuesta, J., Foret, G., Fortems-Cheiney, A., et al. (2018). Lower tropospheric ozone over the North China Plain: Variability and trends revealed by IASI satellite observations for 2008–2016. *Atmospheric Chemistry and Physics*, *18*, 16439–16459. https://doi.org/10.5194/acp-18-16439-2018

EEA report. (2016). *Explaining road transport emissions*. https://doi.org/10.2800/71804

EEA report. (2019). *Air quality in Europe - 2019 report*. https://doi.org/10.2800/822355

EEA report. (2020). *Healthy environment, healthy lives: How the environment influences health and well-being in Europe, 21*. https://doi.org/10.2800/53670

Eskes, H. J., & Boersma, K. F. (2003). Averaging kernels for DOAS total-column satellite retrievals. *Atmospheric Chemistry and Physics*, *3*, 1285–1291. https://doi.org/10.5194/acp-3-1285-2003

Fortems-Cheiney, A., Pison, I., Dufour, G., Broquet, G., Berchet, A., Potier, E., et al. (2019). Variational regional inverse modeling of reactive species emissions with PYVAR-CHIMERE. *Geoscientific Model Development Discussions*. https://doi.org/10.5194/gmd-2019-186

Georgoulias, A. K., van der A, R. J., Stammes, P., Boersma, K. F., & Eskes, H. J. (2019). Trends and trend reversal detection in 2 decades of tropospheric NO_2 satellite observations. *Atmospheric Chemistry and Physics*, *19*, 6269–6294. https://doi.org/10.5194/acp-19-6269-2019

Guenther, A., Karl, T., Harley, P., Wiedinmyer, C., Palmer, P. I., & Geron, C. (2006). Estimates of global terrestrial isoprene emissions using MEGAN (Model of Emissions of Gases and Aerosols from Nature). *Atmospheric Chemistry and Physics*, *6*, 3181–3210. https://doi.org/10.5194/acp-6-3181-2006

ICCT. (2014). *Real-world exhaust emissions from modern diesel cars, International Council on Clean Transportation*. Retrieved from https://theicct.org/sites/default/files/publications/ICCT_PEMS-study_diesel-cars_20141013_0.pdf

IMO International Maritime Organization. (2000). *The international convention for the prevention of marine pollution from ships, 1973 as modified by the protocol of 1978 relating thereto (MARPOL 73/78), Annex VI: Prevention of air pollution from ships, 2008 amendments*.

Jalkanen, J.-P., Brink, A., Kalli, J., Pettersson, H., Kukkonen, J., & Stipa, T. (2009). A modelling system for the exhaust emissions of marine traffic and its application in the Baltic Sea area. *Atmospheric Chemistry and Physics*, *9*, 9209–9223. https://doi.org/10.5194/acp-9-9209-2009

Kendall, M. G. (1975). *Rank correlation methods* (C. Griffin, 4th ed.).

Khaniabadi, Y. O., Goudarzi, G., Daryanoosh, S. M., Borgini, A., Tittarelli, A., & De Marco, A. (2017). Exposure to PM_{10}, NO_2, and O_3 and impacts on human health. *Environmental Science & Pollution Research*, *24*, 2781–2789. https://doi.org/10.1007/s11356-016-8038-6

Krotkov, N. A., McLinden, C. A., Li, C., Lamsal, L. N., Celarier, E. A., Marchenko, S. V., et al. (2016). Aura OMI observations of regional SO_2 and NO_2 pollution changes from 2005 to 2015. *Atmospheric Chemistry and Physics*, *16*, 4605–4629. https://doi.org/10.5194/acp-16-4605-2016

Kuenen, J. J. P., & Dore, C. (2019). *EMEP/EEA guidebook, chapter 5: Uncertainties*. https://doi.org/10.1016/b978-0-12-801238-3.02490-9

Kuenen, J. J. P., Visschedijk, A. J. H., Jozwicka, M., & Denier van der Gon, H. A. C. (2014). TNO-MACC_II emission inventory; a multi-year (2003-2009) consistent high-resolution European emission inventory for air quality modelling. *Atmospheric Chemistry and Physics*, *14*, 10963–10976. https://doi.org/10.5194/acp-14-10963-2014

Kurtenbach, R., Becker, K., Gomes, J., Kleffmann, J., LŽrzer, J., Spittler, M., et al. (2001). Investigations of emissions and heterogeneousformation of HONO in a road traffic tunnel. *Atmospheric Environment*, *35*(20):9506–9517.

Lamsal, L. N., Duncan, B. N., Yoshida, Y., Krotkov, N. A., Pickering, K. E., Streets, D. G., & Lu, Z. (2015). U.S. NO_2 trends (2005-2013): EPA air quality system (AQS) data versus improved observations from the ozone monitoring instrument (OMI). *Atmospheric Environment*, *110*, 130–143. https://doi.org/10.1016/j.atmosenv.2015.03.055

Lattuati, M. (1997). *Impact des émissions européennes sur le bilan de l'ozone troposphérique a l'interface de l'europe et de l'atlantique nord: Apport de la modélisation lagrangienne et des mesures en altitude*, (Ph.D. thesis). Université Paris VI.

Levelt, P. F., Joiner, J., Tamminen, J., Veefkind, J. P., Bhartia, P. K., Stein Zweers, D. C., et al. (2018). The ozone monitoring instrument: Overview of 14 years in space. *Atmospheric Chemistry and Physics*, *18*, 5699–5745. https://doi.org/10.5194/acp-18-5699-2018

Li, J., & Wang, Y. (2019). Inferring the anthropogenic NO_x emission trend over the United States during 2003–2017 from satellite observations: Was there a flattening of the emission trend after the great recession? *Atmospheric Chemistry and Physics*, *19*, 15339–15352. https://doi.org/10.5194/acp-19-15339-2019

Mailler, S., Menut, L., Khvorostyanov, D., Valari, M., Couvidat, F., Siour, G., et al. (2017). CHIMERE-2017: From urban to hemispheric chemistry-transport modeling. *Geoscientific Model Development*, *10*, 2397–2423. https://doi.org/10.5194/gmd-10-2397-2017

MAW, Major Agglomerations of the World. (2020). www.citypopulation.de

Menut, L., Bessagnet, B., Khvorostyanov, D., Beekmann, M., Blond, N., Colette, A., et al. (2013). CHIMERE 2013: A model for regional atmospheric composition modelling. *Geoscientific Model Development*, *6*, 981–1028. https://doi.org/10.5194/gmd-6-981-2013

Menut, L., Bessagnet, B., Mailler, S., Pennel, R., & Siour, G. (2020). Impact of lightning NO_x emissions on atmospheric composition and meteorology in Africa and Europe. *Atmosphere*, *11*, 1128. https://doi.org/10.3390/atmos11101128

Menut, L., Bessagnet, B., Siour, G., Mailler, S., Pennel, R., & Cholakian, A. (2020). Impact of lockdown measures to combat Covid-19 on air quality over western Europe. *Science of the Total Environment*, *741*, 140426. https://doi.org/10.1016/j.scitotenv.2020.140426

Miyazaki, K., Eskes, H., Sudo, K., Boersma, K. F., Bowman, K., & Kanaya, Y. (2017). Decadal changes in global surface NO_x emissions from multi-constituent satellite data assimilation. *Atmospheric Chemistry and Physics*, *17*, 807–837. https://doi.org/10.5194/acp-17-807-2017

Munro, R., Lang, R., Klaes, D., Poli, G., Retscher, C., Lindstrot, R., et al. (2016). The GOME-2 instrument on the Metop series of satellites: Instrument design, calibration, and level 1 data processing–an overview. *Atmospheric Measurements Techniques*, *9*, 1279–1301. https://doi.org/10.5194/amt-9-1279-2016

Ntziachristos, & Samaras (2019). *EMEP/EEA air pollutant emission inventory guidebook 2019, Chapter*. 1.A.3.b.i-iv.road.transport

Owens, R. G., & Hewson, T. (2018). *ECMWF forecast user guide, reading*. https://doi.org/10.21957/m1cs7h

Schenkeveld, V. M. E., Jaross, G., Marchenko, S., Haffner, D., Kleipool, Q. L., Rozemeijer, N. C., et al. (2017). In-flight performance of the ozone monitoring instrument. *Atmospheric Measurements Techniques*, *10*, 1957–1986. https://doi.org/10.5194/amt-10-1957-2017

Schneider, P., Lahoz, W. A., & van der A, R. (2015). Recent satellite-based trends of tropospheric nitrogen dioxide over large urban agglomerations worldwide. *Atmospheric Chemistry and Physics*, *15*, 1205–1220. https://doi.org/10.5194/acp-15-1205-2015

Sen, P. K. (1968). Estimates of the regression coefficient based on Kendall's Tau. *Journal of the American Statistical Association*, *63*, 1379–1389. https://doi.org/10.1080/01621459.1968.10480934

Silvern, R. F., Jacob, D. J., Mickley, L. J., Sulprizio, M. P., Travis, K. R., Marais, E. A., et al. (2019). Using satellite observations of tropospheric NO_2 columns to infer long-term trends in US NO_x emissions: The importance of accounting for the free tropospheric NO_2 background. *Atmospheric Chemistry and Physics*, *19*, 8863–8878. https://doi.org/10.5194/acp-19-8863-2019

Stevens, C. J., David, T. I., & Storkey, J. (2018). Atmospheric nitrogen deposition in terrestrial ecosystems: Its impact on plant communities and consequences across trophic levels. *Functional Ecology*, *32*, 1757–1769. https://doi.org/10.1111/1365-2435.13063

Super, I., Dellaert, S. N. C., Visschedijk, A. J. H., & Denier van der Gon, H. A. C. (2020). Uncertainty analysis of a European high-resolution emission inventory of CO_2 and CO to support inverse modelling and network design. *Atmospheric Chemistry and Physics*, *20*, 1795–1816. https://doi.org/10.5194/acp-20-1795-2020

Szopa, S., Foret, G., Menut, L., & Cozic, A. (2008). Impact of large scale circulation on European summer surface ozone: Consequences for modeling, *Atmospheric Environment*, *43*, 1189–1195. https://doi.org/10.1016/j.atmosenv.2008.10.039

Terrenoire, E., Bessagnet, B., Rouïl, L., Tognet, F., Pirovano, G., Létinois, L., et al. (2015). High-resolution air quality simulation over Europe with the chemistry transport model CHIMERE. *Geoscientific Model Development*, *8*, 21–42. https://doi.org/10.5194/gmd-8-21-2015

van der A, R. J., Eskes, H. J., Boersma, K. F., van Noije, T. P. C., Van Roozendael, M., De Smedt, I., et al. (2008). Trends, seasonal variability and dominant NOx source derived from a ten year record of NO_2 measured from space. *Journal of Geophysical Research*, *113*, D04302. https://doi.org/10.1029/2007jd009021

Visser, A. J., Boersma, K. F., Ganzeveld, L. N., & Krol, M. C. (2019). European NO_x emissions in WRF-Chem derived from OMI: Impacts on summertime surface ozone. *Atmospheric Chemistry and Physics*, *19*, 11821–11841. https://doi.org/10.5194/acp-19-11821-2019

Zara, M., Boersma, K. F., Eskes, H., Denier van der Gon, H., Vilà-Guerau de Arellano, J., Krol, M., et al. (2021). Reductions in nitrogen oxides over the Netherlands between 2005 and 2018 observed from space and on the ground: Decreasing emissions and increasing O_3 indicate changing NO_x chemistry. *Atmospheric Environment*, *9*, 100104. https://doi.org/10.1016/j.aeaoa.2021.100104